JOURNAL OF MATERIALS SCIENCE 32 (1997) 1487–1492

Determination of precipitation–time–temperature (PTT) diagrams for Nb, Ti or V micro-alloyed steels

S. F. MEDINA
Centro Nacional de Investigaciones Metalúrgicas (CENIM-CSIC), Av. Gregorio del Amo 8, 28040 Madrid, Spain

A method is described, developed in CENIM-CSIC, for studying the kinetics of strain induced precipitation in micro-alloyed steels. Using torsion tests, the statically recrystallized fraction has been determined for three Nb, V and Ti micro-alloyed steels at different temperatures and strains. When precipitation starts, the recrystallized fraction deviates from Avrami's equation, making it possible to identify the moment at which precipitation starts (P_s) and finishes (P_f). In this way precipitation–time–temperature (PTT) curves can be drawn, showing the precipitation kinetics in graph form.

1. Introduction

Nb micro-alloyed steels are the most commonly used as the strain induced precipitates are generally smaller than with V or Ti micro-alloyed steels, thus improving their yield strength and ultimate strength [1]. Furthermore, the static recrystallization critical temperature (SRCT), or the temperature at which induced precipitation starts to inhibit recrystallization, is higher in Nb micro-alloyed steels for the same micro-alloy content [2]. In steels with low carbon contents ($<0.15\%$), low Nb contents (around 0.04%) and approximately 80 p.p.m. of N, SRCT is greater than 1000 °C and consequently the interval of temperatures (SRCT-Ar_3) is sufficiently wide, and the application of one or more strains will make it possible to obtain a significant hardening of the austenite (pancaking), and thus a very small ferrite grain, after the austenite (γ) → ferrite (α) transformation [3–7].

A method has recently been developed to simultaneously determine the kinetics of static recrystallization at temperatures above and below SRCT and the kinetics of strain induced precipitation, expressed in precipitation–time–temperature (PTT) diagrams [2, 8–11]. PTT diagrams for micro-alloyed steels have been determined by other authors using theoretical equations [12–15], transmission microscopy [16], or the stress relaxation method [17].

This work uses torsion tests to study the static recrystallization of three micro-alloyed steels with different types of micro-alloy (Nb, V, Ti) and determines the PTT diagrams for each one. The methodology used is described and the results obtained for the three steels are discussed.

2. Experimental procedure

The steels studied were manufactured by electroslag remelting in a laboratory unit capable of producing 30 kg ingots. Their compositions are shown in Table I where it may be seen that their micro-alloy contents are very similar, making it possible to establish specific considerations about their behaviour. The hot torsion tests were carried out using a completely automatic and highly precise machine, whose unit of programmable time for purposes of quantifying the recrystallized fraction was 0.001 s.

The torsion specimens, with a useful length of 50 mm and 6 mm in diameter, were austenitized at 1230 °C for 10 min and rapidly cooled to the testing temperature. It should be noted that at the temperature of 1230 °C the Nb and V precipitates were completely dissolved while Ti nitrides were only partially dissolved.

In order to ensure that the tests were carried out in the austenite phase the Ar_3 temperatures were determined at a cooling rate of 0.2 °C s^{-1} (Table I). The equivalent strains applied were of 0.20 and 0.35 and the strain rate was 3.63 s^{-1}, calculated by the cylindrical surface of the specimen in accordance with Von Mises criterion of yielding [18], whose expressions for stress and for strain are, respectively:

$$\varepsilon = \frac{2\pi R_s N}{(3)^{1/2} L} \tag{1}$$

$$\sigma = \frac{(3)^{1/2} C}{2\pi R_s^3}(3 + m + r) \tag{2}$$

where N = number of turns, C = torque, R_s = radius of specimen and

$$m = \frac{\partial \ln C}{\partial \ln \dot{N}} \quad \text{(strain rate sensitivity)}$$

$$r = \frac{\partial \ln C}{\partial \ln N} \quad \text{(strain hardening exponent)}$$

with $\dot{N}$ being the rotation rate (turns s^{-1}).

0022–2461

TABLE I Chemical composition (wt%), transformation critical temperature (Ar_3; 0.2 °C/s) and austenite grain size (μm) at 1230 °C for 10 min for the steels used

Steel	C	Si	Mn	Nb	V	Ti	N (p.p.m.)	Ar_3 (°C)	D_γ (μm)
Nb	0.11	0.24	1.23	0.042	–	–	112	786	122
V	0.11	0.24	1.10	–	0.043	–	105	784	172
Ti	0.15	0.27	1.15	–	–	0.055	100	779	95

3. Results and discussion

First of all, the austenite grain size of the three steels was measured at the austenitization temperature (1230 °C for 10 min) by means of quenching and subsequent observation with an optical microscope of 20 fields of view, applying the technique of linear intersection. The results are shown in Table I where it can be seen that Ti steel shows the smallest grain size, as was to be expected, given that the inhibiting effect of Ti is known due to the presence of non-dissolved precipitates.

The recrystallized fraction was determined using the method known as "back extrapolation" [19]. Fig. 1 shows the recrystallized fraction against time for Nb steel, determined at a strain of 0.20, strain rate of 3.63 s^{-1} and different temperatures. It may be seen that a plateau starts to form on the curve corresponding to 1025 °C. When it stabilizes the curve adopts the same form as curves obtained at greater temperatures. The plateau is caused by the induced precipitation and its start and finish are identified with the start and finish of induced precipitation [2, 8–11], a fact that will be considered in the construction of the PTT diagrams, as will be seen below. The curves corresponding to temperatures greater than 1025 °C show the same habitual form of Avrami's law for recrystallization. At temperatures below 1025 °C the corresponding curves always show a plateau, whose onset appears at increasingly smaller recrystallized fractions.

Fig. 2 illustrates the recrystallized fraction of V steel for a strain of 0.20 and temperatures of 1100, 1000, 900 and 850 °C, respectively. The curves corresponding to 900 and 850 °C show a plateau caused by the formation of vanadium precipitates which momentarily block the progress of the recrystallization. Fig. 3 shows the recrystallized fraction for Ti steel for a strain of 0.20 and different temperatures. Now the plateau starts to appear on the curve corresponding to 875 °C.

The curves corresponding to a strain of 0.35 presented forms similar to the previous ones (Figs 4–6). Recrystallization is now faster for the same temperature, i.e. the curves shift towards smaller times, it also being possible to see a tendency towards the plateau appearing at slightly lower temperatures. From the above results it may be deduced that induced precipitation occurs in all micro-alloyed steels, whatever their nature, and is capable of momentarily blocking recrystallization. If advantage is taken of this momentary inhibition in rolling, or in any other hot forming process, a highly deformed austenite may be obtained,

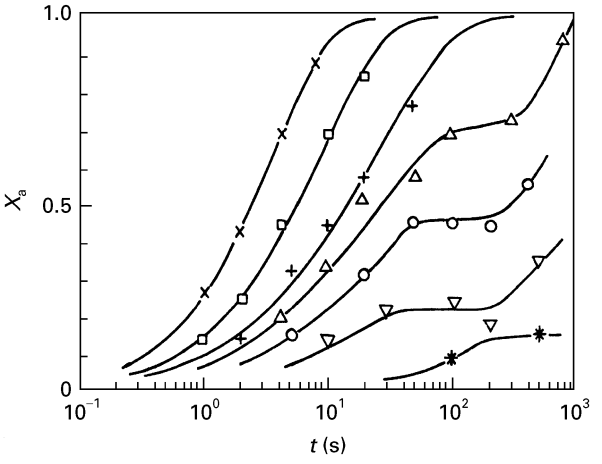

Figure 1 Recrystallized fraction (X_a) versus time for Nb steel. $\varepsilon = 0.20$; $\dot{\varepsilon} = 3.63\ s^{-1}$. Key: × 1150 °C; □ 1100 °C; + 1050 °C, △ 1025 °C; ○ 1000 °C; ▽ 975 °C; ∗ 950 °C.

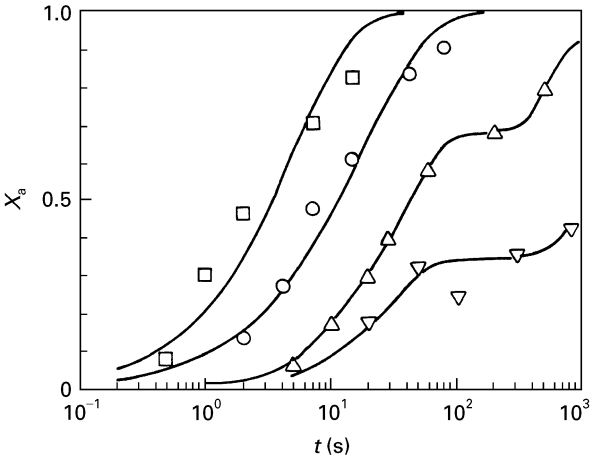

Figure 2 Recrystallized fraction (X_a) versus time for V steel. $\varepsilon = 0.20$; $\dot{\varepsilon} = 3.63\ s^{-1}$. Key: □ 1100 °C; ○ 1000 °C; △ 900 °C; ▽ 850 °C.

and thus a very fine ferrite grain size after the $\gamma \rightarrow \alpha$ transformation.

It should be noted that the plateau has been determined with precision thanks to the use of the back extrapolation method for determining the recrystallized fraction. If we had used the technique of double deformation, which determines the total softened fraction, i.e. the recovery plus the recrystallized fraction, the incubation time of the latter would appear as a plateau formed after the finalization of softening due to the recovery; i.e. there would be a double plateau and a possible overlapping of the two [20, 21].

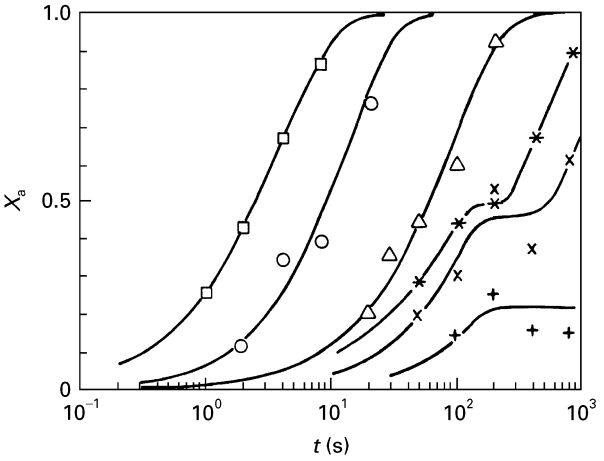

Figure 3 Recrystallized fraction (X_a) versus time for Ti steel, $\varepsilon = 0.20$; $\dot{\varepsilon} = 3.63\ s^{-1}$. Key: □ 1100 °C; ○ 1000 °C; △ 900 °C; ∗ 875 °C; × 850 °C; + 825 °C.

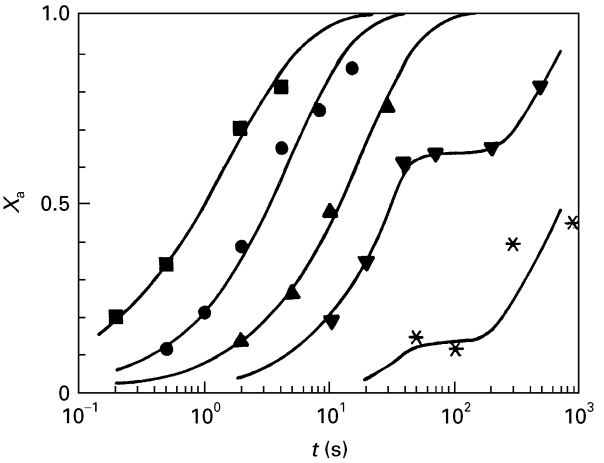

Figure 5 Recrystallized fraction (X_a) versus time for V steel. $\varepsilon = 0.35$; $\dot{\varepsilon} = 3.63\ s^{-1}$. Key: ■ 1100 °C; ● 1000 °C; ▲ 900 °C; ▼ 850 °C; ∗ 825 °C.

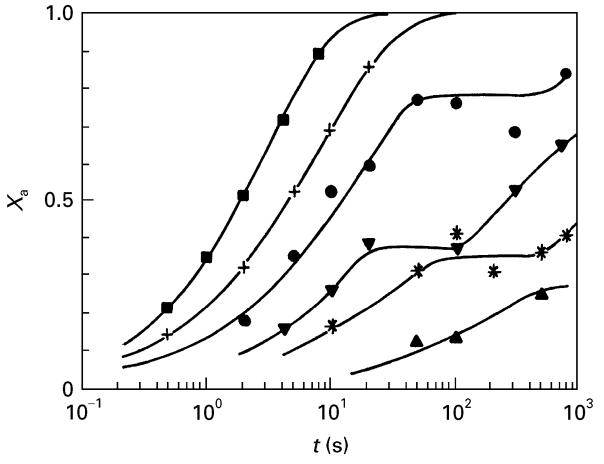

Figure 4 Recrystallized fraction (X_a) versus time for Nb steel, $\varepsilon = 0.35$; $\dot{\varepsilon} = 3.63\ s^{-1}$. Key: ■ 1100 °C; + 1050 °C; ● 1000 °C; ▼ 975 °C; ∗ 950 °C; ▲ 900 °C.

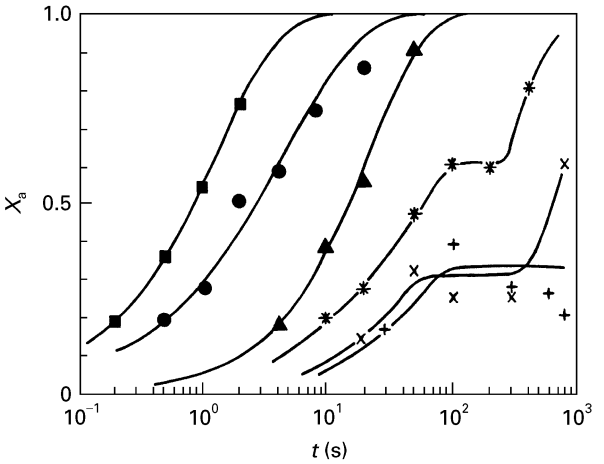

Figure 6 Recrystallized fraction (X_a) versus time for Ti steel, $\varepsilon = 0.35$; $\dot{\varepsilon} = 3.63\ s^{-1}$. Key: ■ 1100 °C; ● 1000 °C; ▲ 900 °C; ∗ 875 °C; × 850 °C; + 825 °C.

The kinetics of the static recrystallization of austenite can be described by an Avrami equation in the following way:

$$X_a = 1 - \exp\left[-0.693\left(\frac{t}{t_{0.5}}\right)^n\right] \qquad (3)$$

where X_a is the fraction of the recrystallized volume and $t_{0.5}$ is the time corresponding to half of the recrystallized volume, which depends practically on all the variables which intervene in hot deformation and whose most general expression follows a law of the type:

$$t_{0.5} = A\varepsilon^p \dot{\varepsilon}^q D^s \exp\frac{Q}{RT} \qquad (4)$$

where ε is the strain, $\dot{\varepsilon}$ is the strain rate, D is the grain size, Q is the activation energy, T is absolute temperature, $R = 8.318\ J\ mol^{-1}\ K^{-1}$ and p, q and s are parameters.

Thus, from Equation 4 it is deduced that the logarithmic representation of $t_{0.5}$ against the inverse of the absolute temperature ($1/T$) makes it possible to determine the activation energy (Q) for static recrystallization. Fig. 7 shows an example, specifically for Nb steel, where the values of $t_{0.5}$ have been represented for the two strains. The activation energy is given by the slope of each curve multiplied by the constant R. Before the start of induced precipitation the activation energy is seen to be constant, with a value of 262 000 J mol^{-1} corresponding to the linear section of the curve, and below a certain temperature, referred to above as SRCT, the activation energy comes to be a function of the temperature, coinciding with the non-linear section. From the parallelism of the two straight lines it is deduced that the activation energy is independent of the strain. The values of Q for V and Ti steels, in the temperature intervals where it is constant, were 166 000 J mol^{-1} and 205 000 J mol^{-1}, respectively.

A further representation of Q, also against $1/T$, will make it possible to finally calculate the value of SRCT for each steel, strain and austenite grain size. Fig. 8 shows an example, also for Nb steel, where it can be seen that a greater strain reduces the value of SRCT, given by the intersection of the horizontal line with the sloping line. In the same way SRCT was determined

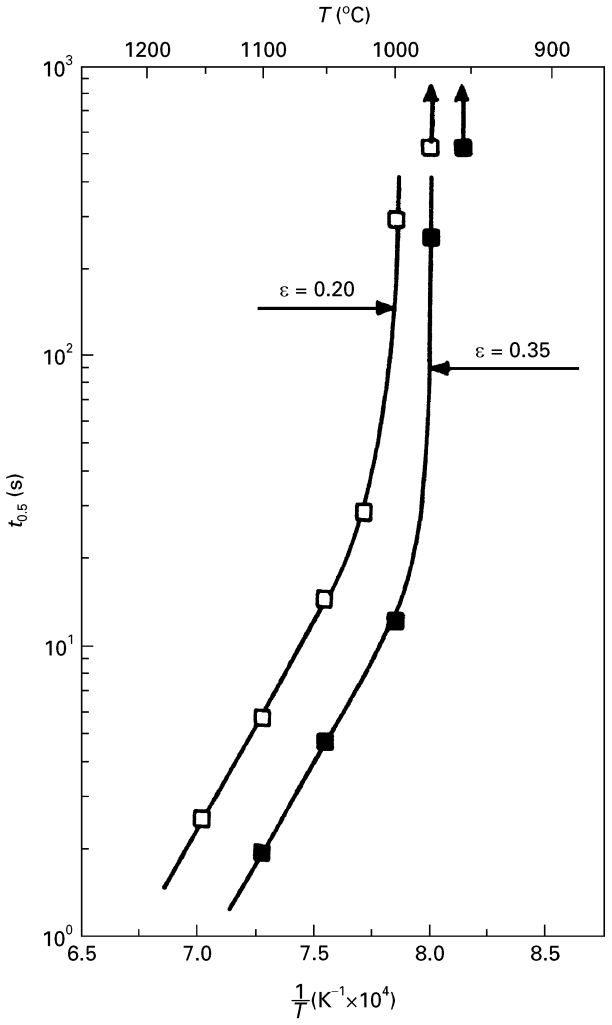

Figure 7 Plot of $t_{0.5}$ against the reciprocal of the temperature for Nb steel.

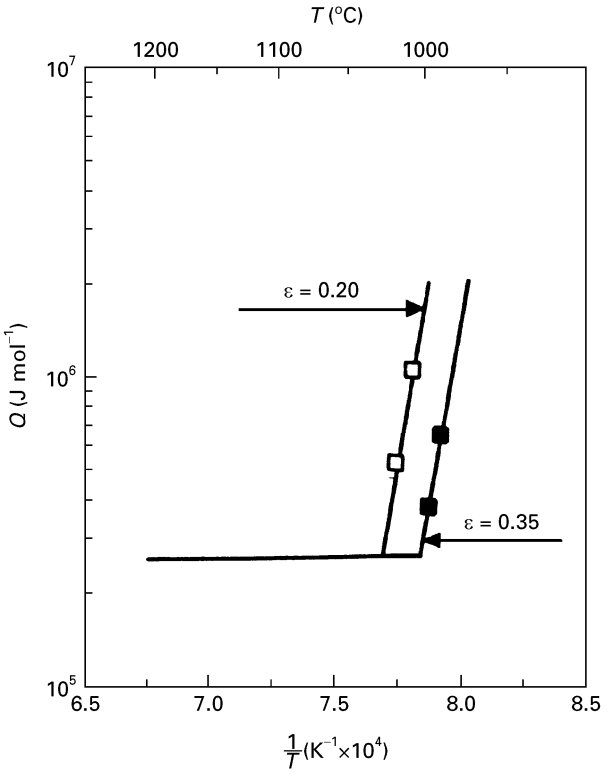

Figure 8 Plot of the activation energy (Q) against the reciprocal of the temperature for Nb steel.

TABLE II Static recrystallization critical temperature (SRCT) and solubility temperature (nitrides and carbides) for the steels used

Steel	SRCT (°C) ε = 0.20	SRCT (°C) ε = 0.35	Precipitate: T_s (°C)
Nb	1030	1005	NbN: 1114 [22] NbC: 1095 [22]
V	903	880	VN: 974 [22] VC: 777 [22]
Ti	908	897	TiN: 1550 [23] TiC: 1068 [22][a]

[a] Calculated with Ti dissolved (0.022, wt %) at 1230 °C for 10 min.

for V and Ti steels, and these values are shown in Table II. A comparison of the values of SRCT with the temperatures deduced from the products of solubility [22, 23] makes it possible to deduce with good approximation the chemical nature of the precipitates (Table II) responsible for the inhibition of static recrystallization. Thus, in Nb steel the precipitates are niobium carbonitrides, though possibly the character of nitride is preponderant. In V steel they are nitrides, as carbides would form at much lower temperatures. In Ti steel there are nitrides formed at temperatures close to solidification temperatures, but the strain induced precipitates responsible for the inhibition of recrystallization are carbides. This is obvious if we consider that the Ti in solution at 1230 °C for 10 min was approximately 0.022% [23] and therefore the Ti still precipitated at this temperatures was 0.029%. The stoichiometric relation (Ti/N = 3.4) of the titanium nitrides (TiN) indicates that practically all the nitrogen is formally precipitated at the austenitization temperature and therefore the Ti in solution and subsequently precipitated by the effect of the strain is carbides. Obviously, SRCT is lower in all cases than the solubility temperature, as the strain induced precipitation moves away from the thermodynamic conditions of equilibrium with which the solubility products have been determined.

The values in Table II indicate that for the same micro-alloy content, Nb micro-alloyed steels present the greatest SRCT, offering greater facilities for the "pancaking" of the austenite during the course of rolling.

From the curves which present a plateau (Figs 1–6) it is possible to deduce the start (P_s) and finish times (P_f) of induced precipitation, which will allow us to draw the PTT diagrams. Fig. 9 shows the PTT diagram for Nb steel, it being seen that the minimum incubation time, which corresponds to the nose of the curve, depends on the strain. It should be noted that the asymptote of the curves P_s and P_f is the horizontal line defined by SRCT and this is a great help in their plotting. It is seen that an increase in the strain reduces the incubation time, though it is known that this influence is conditioned on the Nb content, being smaller as the Nb content increases [9]. Fig. 10 shows the PTT diagram for V steel. The substantial difference compared with the previous diagram (Nb steel) is

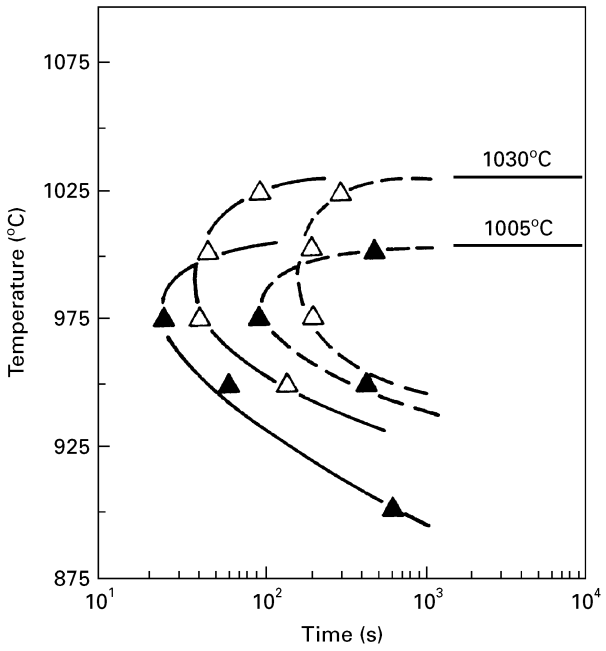

Figure 9 PTT diagrams for Nb steel. Key: △ ε = 0.20; ▲ ε = 0.35; —— P_s; – – – P_f.

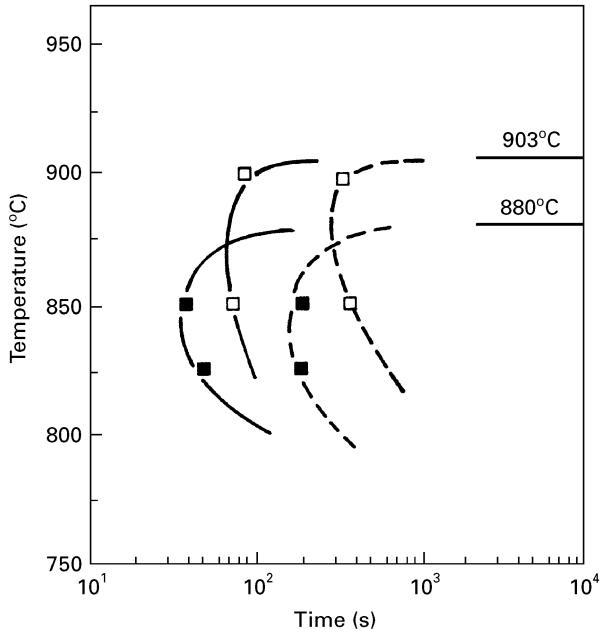

Figure 10 PTT diagrams for V steel. Key: □ ε = 0.20; ■ ε = 0.35; —— P_s;– – –P_f.

the lower value of SRCT and consequently the lower temperature of the nose of the curve (NT). Fig. 11 illustrates the PTT diagram for Ti steel, it being seen that the incubation times for the titanium carbides are greater than for the vanadium nitrides and niobium carbonitrides. Table III displays the values of NT and the minimum values of P_s, corresponding to the nose of the curve. The influence of the micro-alloy content has been studied elsewhere [8–11] and an increase tends to reduce the incubation time of the precipitation. This may explain why P_s for Ti steel is much greater than for steels Nb and V, as the Ti content in solution at 1230 °C for 10 min was, as has been mentioned above, 0.022 (wt %), less than the quantities of Nb (0.042) or V (0.043). Nevertheless, Nb steel presented lower P_s than the V steel and this indicates that though the precipitation kinetics are qualitatively similar the incubation times also depend not only on the micro-alloy content but also on the nature of the micro-alloy.

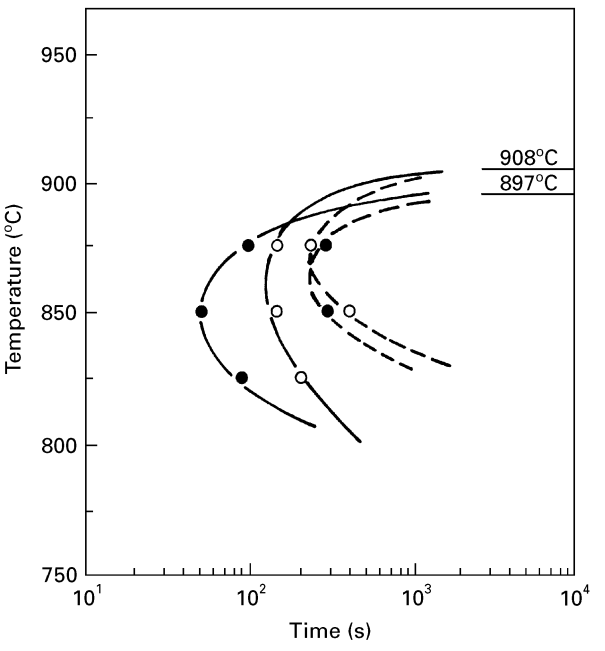

Figure 11 PTT diagrams for Ti steel. Key: ○ ε = 0.20; ● ε = 0.35; —— P_s; – – – P_f.

TABLE III Experimental values of nose temperature (NT) and minimum incubation (P_s) time of the precipitates, for the steels used

Steel	Minimum P_s (s)		NT (°C)	
	ε = 0.20	ε = 0.35	ε = 0.20	ε = 0.35
Nb	40	25	990	975
V	70	40	865	845
Ti	130	50	862	850

4. Conclusions

1. The method presented makes it possible to determine the PTT diagrams and thus to know the kinetics of precipitation.
2. For the same micro-alloy content Nb steels present higher values of SRCT.
3. In spite of the low percentage of Ti in solution at 1230 °C for 10 min, around 0.022%, Ti steel presents an SRCT close to that of V steel due to Ti's great affinity to carbon.
4. Small amounts of micro-alloy are sufficient to form precipitates.
5. An increase in the strain reduces the incubation time of the precipitates.
6. The incubation time also depends on the nature of the precipitates.

Acknowledgements

The author is grateful for the financial support of CICYT of Spain.

References

1. T. GLADMAN, *Ironmaking Steelmaking* **16** (1989) 241.
2. S. F. MEDINA and J. E. MANCILLA, *ISIJ Int.* **33** (1993) 1257.
3. S. F. MEDINA and V. LÓPEZ, *ibid.* **33** (1992) 614.
4. A. NAJAFI-ZADEH, S. YUE and J. J. JONAS, *ibid.* **32** (1992) 213.
5. L. N. PUSSEGODA and J. J. JONAS, *ibid.* **31** (1991) 278.
6. F. H. SAMUEL, S. YUE, J. J. JONAS and B. A. ZBINDEN, *ibid.* **29** (1989) 878.
7. F. H. SAMUEL, S. YUE, J. J. JONAS and K. R. BARNES, *ibid.* **30** (1991) 216.
8. S. F. MEDINA and J. E. MANCILLA, *Scripta Metall. Mater.* **30** (1994) 73.
9. *Idem*, *Acta Metall. Mater.* **42** (1994) 3945.
10. S. F. MEDINA, J. E. MANCILLA and C. A. HERNÁNDEZ, *ISIJ Int.* **34** (1994) 689.
11. S. F. MEDINA and J. E. MANCILLA, *Scripta Metall. Mater.* **31** (1994) 315.
12. B. DUTTA and C. M. SELLARS, *Mater. Sci. Technol.* **3** (1987) 197.
13. S. OKAGUCHI and T. HASHIMOTO, *ISIJ Int.* **32** (1992) 283.
14. S. H. PARK, S. YUE and J. J. JONAS, *Metall. Trans. A* **23A** (1992) 1641.
15. D. Q. BAI, S. YUE, W. P. SUN and J. J. JONAS, *Metall. Trans. A* **24A** (1993) 2151.
16. A. LE BON, J. ROFES-VERNIS and C. ROSSARD, *Met. Sci.* **9** (1975) 36.
17. W. J. LIU and J. J. JONAS, *Metall. Trans. A* **20A** (1989) 1361.
18. A. FAESSEL, *Rev. Métal. CIT.* **4** (1976) 875.
19. H. L. ANDRADE, M. G. AKBEN and J. J. JONAS, *Metall. Trans. A* **14A** (1983) 1967.
20. R. A. PETROVIC, M. J. LUTON and J. J. JONAS, *Can. Metall. Q.* **14** (1975) 137.
21. R. A. P. DJAIC and J. J. JONAS, *Metall. Trans.* **4** (1973) 621.
22. K. NARITA, *Trans. Iron Steel Inst. Jpn.* **15** (1975) 145.
23. E. T. TURKDOGAN, *Iron Steelmaker* **16** (1989) 61.

Received 19 January
and accepted 17 September 1996